DOI: 10.1002/fuce.201600044

Density Functional Theory Study of Ni Clusters Supported on the ZrO_2(111) Surface▲

A. Cadi-Essadek[1], A. Roldan[2], N. H. de Leeuw[1,2]*

[1] Department of Chemistry, University College London, 20 Gordon Street, London, WC1H 0AJ, United Kingdom
[2] School of Chemistry, Cardiff University, Main Building, Park Place, CF10 3AT, Cardiff, United Kingdom

Received March 04, 2016; accepted November 14, 2016; published online December 16, 2016

Abstract

The nickel/zirconia (Ni/ZrO_2) interface plays a key role in the performance of the anode of solid oxide fuel cells (SOFC) and it is therefore important to understand the interaction between nickel nanoparticles and the ZrO_2 surface. Here, we have described the interaction of five Ni_n (n = 1–5) clusters with the (111) surface of cubic zirconia, c-ZrO_2(111), using spin polarized density functional theory (DFT) calculations with inclusion of long-range dispersion forces. We have systematically evaluated the geometric and electronic structure of different cluster configurations and sizes and shown how the clusters interact with the oxygen and zirconium surface atoms. The cluster-surface interaction is characterized by a charge transfer from the Ni clusters to the surface. From calculations of the hopping rate and clustering energies, we have demonstrated that Ni atoms prefer to aggregate rather than wet the surface and we would therefore suggest that modifications in the synthesis could be needed to modify the coalescence of the supported metal particles of this catalytic system.

Keywords: *Ab-initio* Calculations, Fuel Cells, Hopping Rate, Oxide Surface Supported Cluster, Zirconia

1 Introduction

Metal-oxide interfaces are efficient catalytic systems used in many industrial processes, e.g., microelectronics, sensors and solid oxide fuel cells (SOFC) [1–7], hence the growing interest in these cermets over the past decade. SOFC are electrochemical devices which convert chemical energy into electrical energy [8, 9], but robust materials are needed since they operate under a high working temperature of approximately 500–900 °C [10, 11]. A suitable candidate material is zirconia (ZrO_2) since it has low thermal conductivity, high fracture toughness and bulk modulus, in addition to being chemically inert and corrosion resistant [3, 12]. Doping cubic zirconia (c-ZrO_2) with yttria (Y_2O_3) stabilizes the cubic zirconia polymorph at low temperatures and makes it more suitable for use as an anode in the SOFC. Indeed, ytrria-stabilized zirconia (YSZ) has a higher oxygen-ion conductivity and is stable under both oxidizing and reducing conditions [13].

Nickel is the metal primarily used in SOFC, and it is well known that the performance of the Ni/YSZ cermet depends on the microstructure and the distribution of the Ni and YSZ phases in the cermet [14]. This performance depends also on the key reactions occurring at the triple phase boundary (TPB) where the gas phase, Ni particles and YSZ surface meet. Therefore, the catalytic activity of the surface is directly linked to the nature of the metal-support interaction [2] and hence our interest in Ni/ZrO_2 interface.

Methods based on the density functional theory (DFT) are suitable for the description of metal-oxide interfaces [15], but it is a time-consuming method and in this work we have therefore focused on the study of the adsorption of small clusters (Ni_{1-5}) on the ZrO_2(111) surface to provide fundamental insight into the Ni/ZrO_2(111) interaction. Other authors have used DFT to study related metal-oxide interfaces. For instance, Catlow et al. [2] have investigated the deposition of palladium

▲ *Paper presented at the 6th International Conference on Fundamentals and Development of Fuel Cells (FDFC2015), February 3 – 5, 2015 held in Toulouse, France.*

[*] *Corresponding author, DeLeeuwN@cardiff.ac.uk*

This is an open access article under the terms of the Creative Commons Attribution License, which permits use, distribution and reproduction in any medium, provided the original work is properly cited.

and platinum layers on zirconia and ceria surfaces and found that the electronic configuration of the noble metal is determined by the metal support interaction. Li et al. [16] studied the deposition of an Au_{10} cluster on the MgO(111) surface and demonstrated charge transfer from the cluster to the surface. Teng et al. [15] deposited Au_x (x = 1–10) on the stoichiometric and partially reduced CeO_2(111) surfaces and showed that the stability of Au_x clusters depends on the surface structure and the Au-Au bond strength and arrangement. Jiang et al. [17] used DFT to investigate the geometric structure of Pt_n (n = 4–8) clusters on the TiO_2(110) surface. They found that Pt_4 adopts a flat geometry upon adsorption, while Pt_n (n = 5–8) adopts a two-layer structure where only the bottom layer interacts with the support. Luches et al. [18] characterized by STM and XPS measurements the nucleation and growth of Ag nanoparticles on CeO_2(111). They have also complemented their experimental results with DFT calculations, where they showed charge transfer from the Ag clusters to the ceria surface. Hahn et al. [19] used DFT to study the adsorption of Ni clusters on top of CeO_2(111) and showed that the metal cluster is stabilized as the cluster size increases (up to ten atoms). Ma et al. [20], in their investigation of the nucleation and aggregation processes of Ag atoms on the AgCl(100) surface, demonstrated that the clusters are thermodynamically more stable than layered structures with the stability increasing with the cluster size. Jung et al. [21] described the interaction of CO with M (M = Pd and Pt) supported on c-ZrO_2(111), although these authors were more focused on the effect of M/ZrO_2(111) on CO adsorption rather than on the M-ZrO_2 interaction itself.

A systematic study of the influence of Ni cluster size and configuration on the Ni/ZrO_2 interface is still lacking and in this work we have therefore analyzed the interaction of 5 Ni_n (n = 1–5) clusters with the c-ZrO_2(111) surface, showing the effect of the cluster configuration on the binding process. We have also analyzed the electronic structure of the Ni_n/ZrO_2(111) interface to describe the electronic rearrangement of the surface atoms caused by the metal cluster. Finally, we have calculated the hopping rate to gain insight into the diffusion of Ni atoms on the c-ZrO_2(111) surface.

2 Models and Computational Methods

We have performed the DFT [22] calculations using the Vienna Ab-initio Simulation Package (VASP) [23–26] which solves the Kohn-Sham equations in a periodic approximation. The exchange-correlation functional was approximated using the generalized gradient approximation (GGA) [27] with the Perdew-Burke-Ernzerhof (PBE) density functional. The long-range dispersion interactions were described by the semi-empirical method of Grimme [28]. The O (2 s, 2 p), Ni (3 d, 4 s) and Zr (4 d, 5 s) atomic orbitals have been treated as valence electrons and their interaction with the remaining frozen core electrons was described by the projected augmented wave method (PAW) [29]. To determine the number of plane-waves a kinetic energy cutoff was set at 500 eV and all the calculations were spin polarized. To optimize the geometry of the system, a conjugate gradients technique was adopted with an interatomic force threshold of 0.01 eV $Å^{-1}$. For the ZrO_2 bulk calculations the reciprocal space was described by Monkhorst-Pack grids with 9 × 9 × 9 mesh of k-points. For the 1 × 1 slab calculations a 7 × 7 × 1 mesh of *k*-points was used, while for the 2 × 2 slab calculations a 3 × 3 × 1 mesh of *k*-points was adopted.

The space group of cubic zirconia (c-ZrO_2) is Fm3m with a face-centered cubic (fcc) unit cell (fluorite crystal structure). The fcc cube is formed by the Zr atoms which are each coordinated to eight oxygen atoms. The position of the O atoms is on the diagonals of the cube. The METADISE code [30] was used to generate the ZrO_2(111) surface, where the atomic charges and the periodicity in the plane direction are taken into account. This code allowed us to obtain a stacking of the atomic layers resulting in a zero dipole moment perpendicular to the surface plane, although this particular surface we could also have obtained by using the electron counting method [31]. Different surface terminations have been investigated and the most stable determined here was the O-terminated ZrO_2(111), in agreement with previous studies [1, 32].

A slab model was considered to define the surfaces and the vacuum size was set to 15 Å in order to avoid perpendicular interactions. Nine atomic layers (three O–Zr–O trilayers) in the z-direction were adopted for the slab thickness. The top five atomic layers were allowed to relax during geometry optimization, while the bottom four layers were kept fixed at their bulk equilibrium position to represent the rest of the crystal. For the adsorption of one Ni atom on the surface, a 1 × 1 slab was considered, which contains 36 atoms (four atoms per atomic layer) and has a surface area of 44.96 $Å^2$. When we adsorbed more than one Ni on the surface, a 2 × 2 slab was considered to avoid lateral interactions between Ni clusters. Thus, the 2 × 2 slab contains 144 atoms (sixteen atoms per atomic layer) and has a surface area of 179.84 $Å^2$.

To describe the interaction of the Ni clusters with the surface we have calculated the clustering energy per Ni atom as follow (Eq. (1)):

$$E_{clus} = \frac{E_{Ni_n/ZrO_2} - (E_{ZrO_2} + nE_{Ni})}{n} \quad (1)$$

where E_{Ni_n/ZrO_2}, E_{ZrO_2} and E_{Ni} are the energies of the slab with the n Ni atoms adsorbed on the surface, the clean oxide ZrO_2 surface and the Ni metal atom, respectively, and n is the number of adsorbed Ni atoms. A positive clustering energy means that Ni atoms prefer to aggregate rather than wet the surface, whereas a negative clustering energy indicates that the Ni atoms prefer to spread over the surface.

We have also calculated the cohesive energy of the metal cluster configurations (Eq. (2)):

$$E_{coh} = \frac{E_{Ni_n} - nE_{Ni}}{n} \quad (2)$$

where E_{Ni_n} is the energy of the Ni_n cluster. To calculate E_{Ni_n} we first optimized Ni_n/ZrO_2, then removed the surface and

 © 2017 The Authors. Published by WILEY-VCH Verlag GmbH & Co. KGaA, Weinheim

performed a single point calculation of the Ni_n geometry as in the optimized Ni_n/ZrO_2 system. Finally, we have described the perpendicular interactions between the surface and the Ni clusters from the interaction energy (Eq. (3)):

$$E_{\text{int}} = \frac{E_{Ni_n/ZrO_2} - (E'_{ZrO_2} + E_{Ni_n})}{n_c} \quad (3)$$

where E'_{ZrO_2} is the energy of the geometry of the clean ZrO_2 surface taken from the optimized Ni_n/ZrO_2 structure and n_C is the number of Ni atoms in contact with the surface. To calculate E'_{ZrO_2}, we first optimized Ni_n/ZrO_2, then removed the Ni_n cluster and performed a single point calculation of the ZrO_2 geometry as it is in the optimized Ni_n/ZrO_2 system.

3 Results and Discussion

Before generating the surface, we calculated the c-ZrO_2 cell parameter at 5.095 Å, in good agreement with experimental results and previous first principles quantum mechanical calculations [33, 34]. The surface energy (1.20 J m^{-2}) of our O-terminated ZrO_2(111) optimized surface also agrees with other investigations [1, 35–37].

3.1 Structural Analysis of the Ni-surface Interface

3.1.1 Ni_1/ZrO_2(111)

We first studied the adsorption of one Ni atom on the ZrO_2(111) surface, before building up the Ni_n clusters and investigating their interaction with the zirconia surfaces. We considered seven different initial adsorption sites for the Ni atom on the O-terminated ZrO_2(111): the Zr atom, the topmost oxygen O_u (up) (located in the top oxygen layer), O_d (down) (located in the lower oxygen layer of the uppermost ZrO_2 trilayer), the position between each pair of sites (O_u–Zr, O_u–O_d and O_d–Zr) and finally above the center of the O_u–O_d–Zr "triangle" (Figure 1).

The clustering energy was calculated for each initial adsorption site and ranged from 2.42 eV on the O_u–O_d–Zr to 3.76 eV for the Zr initial positions. Ni adsorbs preferentially on top of O_d' (slightly off from the perpendicular) since it has the lowest (least positive) clustering energy (2.42 eV) for this site. From Figure 2, we note that Ni interacts with the two nearest O_u atoms causing a movement of those two surface atoms away from their initial positions. Indeed, the O_u–O_u distance is 3.603 Å for the clean surface, which becomes 3.708 Å upon Ni adsorption due to the interaction between Ni and the oxygen surface.

The analysis of the Bader charges (Table 1) shows the effect of Ni on the electronic structure of the surface atoms. Upon

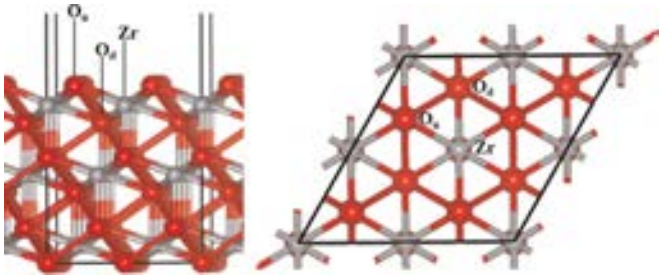

Fig. 1 Side and top views of the O-terminated ZrO_2(111) surface showing the initial adsorption sites for Ni. Color key: red and gray spheres represent oxygen and zirconium atoms, respectively.

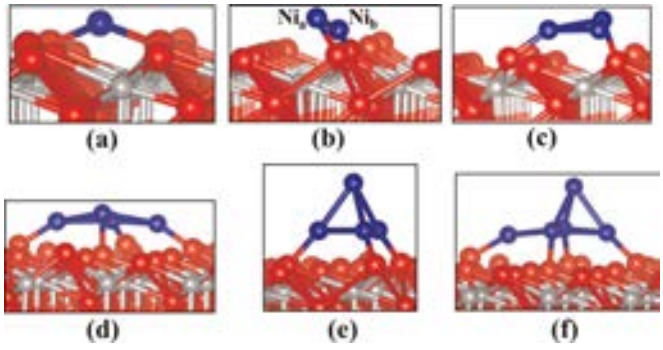

Fig. 2 (a), (b), (c), (d), (e) and (f) side view of Ni_1/ZrO_2(111), Ni_2/ZrO_2(111), Ni_3/ZrO_2(111), flat-Ni_4/ZrO_2(111), pyr-Ni_4/ZrO_2(111) and Ni_5/ZrO_2(111) systems, respectively. Color key: red, gray, and blue spheres correspond to oxygen, Zr and Ni atoms, respectively.

Table 1 Calculated energies, charges and d-band center position for the most stable configuration of the 5 systems.

energies / eV					
	Ni_1/ZrO_2(111)	Ni_2/ZrO_2(111)	Ni_3/ZrO_2(111)	flat-Ni_4/ZrO_2(111)	Ni_5/ZrO_2(111)
E_{clus}	2.42	2.16	1.77	1.57	1.53
E_{coh}	–	3.83	3.38	3.11	2.88
E_{int}	–3.80	–2.38	–2.16	–2.04	–2.05
			bader charge / e$^-$		
	Ni_1/ZrO_2(111)	Ni_2/ZrO_2(111)	Ni_3/ZrO_2(111)	Flat-Ni_4/ZrO_2(111)	Ni_5/ZrO_2(111)
Ni	0.3	0.2	0.3	0.4	0.4
			d-band center		
	Ni_1/ZrO_2(111)	Ni_2/ZrO_2(111)	Ni_3/ZrO_2(111)	Flat-Ni_4/ZrO_2(111)	Ni_5/ZrO_2(111)
Ni	–0.55	–1.18	–1.18	–1.29	–1.73

 © 2017 The Authors. Published by WILEY-VCH Verlag GmbH & Co. KGaA, Weinheim

adsorption, the charge of the O_u and Zr atoms nearest the Ni is modified, from –1.2 to –1.1 e^- and from 2.3 e^- to 2.1 e^- for O_u and Zr, respectively. Ni has obtained a charge of +0.3 e, showing a slight oxidation of metallic Ni due to the charge transfer to the surface, which causes the electronic rearrangement of the O_u and Zr atoms.

We have plotted the electron density difference as $\Delta\rho = \rho_{(Ni/surface)} - (\rho_{(surface)} + \rho_{(Ni)})$ in Figure 3, showing the orientation of the atomic orbitals, from which a gain of electron density between Ni and the surface atoms is clearly seen. For instance, a charge accumulation is observed between the Ni and Zr atoms, confirming the electronic rearrangement described by the Bader analysis, with the atomic orbitals of O_u atoms pointing towards the Ni adatom. In addition, Figure 3 displays charge depletion around the Ni atom.

3.1.2 $Ni_n/ZrO_2(111)$

As it is difficult to consider all possible configurations of the Ni_n clusters, we will build the clusters incrementally with the shape and the initial adsorption sites based on our $Ni_1/ZrO_2(111)$ findings above and previous investigations in the literature of similar systems, i.e., metal clusters supported on oxide materials [16, 20, 21, 38].

We identified in the previous section that Ni is preferentially positioned on top of the O_d' site, where it interacts mainly with its nearest O_u and Zr neighbors. Therefore, the atoms of the cluster facing the surface are initially positioned near the O_u atoms and on top of the O_d' site. The other consideration taken into account in the $Ni_n/ZrO_2(111)$ interfaces is the cluster shape. Since in the metal, the Ni(111) is the most stable surface [39, 40], Ni(111)-facetted clusters have been adsorbed on the metal oxide surface. Thus, the initial atomic spacing in the Ni_n clusters corresponds to the one in the Ni(111) metal surface, i.e., 2.2 Å, although all atoms in the Ni clusters as well as the surface zirconia layers are allowed to move and relax freely during the geometry optimization .

The first cluster studied here is Ni_2 which adsorbs on the $ZrO_2(111)$ surface with a clustering energy of 2.16 eV. Ni_a and Ni_b (Figure 2 (b)) were initially positioned at 2.650 Å and 2.466 Å, respectively, from their nearest O_u neighbor. After geometry optimization, we note a decrease of the Ni–O_u distance: Ni_a–O_u = 1.753 Å and Ni_b-O_u = 1.813 Å. Additionally, each O_u has moved away from its initial position, similar to the observation made for $Ni_1/ZrO_2(111)$: the final O_u–O_u distance observed for $Ni_2/ZrO_2(111)$ is 4.621 Å whereas it is 3.603 Å for the clean surface. This effect of the interaction of Ni_2 with surface atoms can be confirmed further by evaluating the charge of the cluster and the relevant surface atoms.

The analysis of the Bader charges shows a decrease of 0.1 e^- in the negative charge of both O_u atoms interacting with Ni_2. The positive charge of the Zr atom is decreased by 0.2 e^- and the sum of the cluster charge is +0.2 e. This electronic rearrangement is visualized in the electron density difference plot (Figure 3) where we have an obvious charge accumulation between Ni_2 and the surface. In addition, the orbitals of the two O_u interacting with the adatoms are well localized and pointing towards Ni.

The second cluster considered here is $Ni_3/ZrO_2(111)$ where the cluster adsorbs on the surface with a clustering energy of 1.77 eV. After geometry optimization, the final shape of the Ni_3 cluster is a triangle where each Ni interacts with its nearest O_u neighbors, similarly to the metal-surface interactions of the Ni_1 and Ni_2 clusters. Each Ni atom is positioned at 1.8 Å from its nearest O_u neighbor, whereas before geometry optimization the average Ni-O_u distances was 2.3 Å. We also observe in the $Ni_3/ZrO_2(111)$ system a shift of the O_u atom positions, in the surface plane, as was found for $Ni_1/ZrO_2(111)$ and $Ni_2/ZrO_2(111)$. Moreover, the center of the Ni_3 triangle is positioned over the Zr surface atom to optimize the interaction with it. This interaction is confirmed by the Bader charge analysis, since the charge on this Zr atom is +2.0 e while it is +2.3 e for the clean surface. We also note an average decrease of 0.1 e^- in the negative charge of the O_u atoms (nearest neighbors of Ni) upon Ni_3 adsorption: –1.1 e^- for $Ni_3/ZrO_2(111)$ while it is –1.2 e^- for the clean $ZrO_2(111)$ surface. Finally, the total charge of the Ni_3 cluster is +0.3 e , indicating that charge transfer to the surface takes place, which explains the electronic rearrangement observed for O_u and Zr.

The analysis of the electron density difference plot (Figure 3) shows this modest charge transfer from Ni_3 cluster to the surface, since we observe an accumulation of charge between the cluster and the Zr atom located under the cluster. Another accumulation of charge is observed between each Ni atom and its nearest O_u neighbor, whereas in the

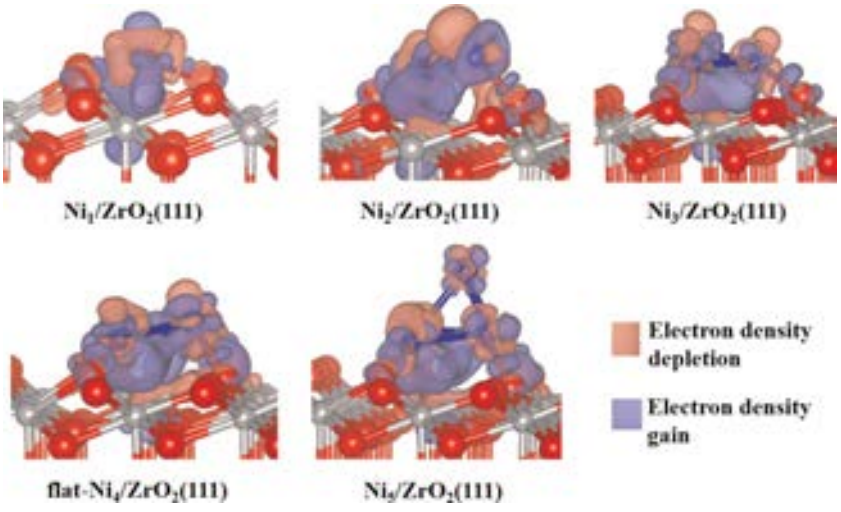

Fig. 3 Calculated electron density difference for the most stable configuration of the 5 systems. Color key: red, gray, and blue spheres correspond to oxygen, Zr and Ni atoms, respectively. Isosurface level: 0.005

 © 2017 The Authors. Published by WILEY-VCH Verlag GmbH & Co. KGaA, Weinheim

meantime a depletion of charge is observed around each Ni atom.

The third cluster considered in this investigation is Ni_4/ZrO_2(111) where the clustering energy of the most stable configuration (Figure 2 (d)) is 1.57 eV. This flat configuration is slightly more favorable than the pyramid one (Figure 2 (e), 1.62 eV), since in flat-Ni_4/ZrO_2(111) the Ni–O_u interactions are maximized which stabilizes the Ni_4 cluster. In terms of the total energy, the flat configuration is 0.23 eV more stable than the three dimensional cluster. Indeed, in the flat configuration we have 4 Ni interacting with 4 O_u while in the pyramid shape only 3 O_u are involved in the interaction with the Ni_4 cluster. Thus, we focus here only on the flat shape and it can be seen from Figure 2 (d) that upon adsorption the nearest O_u atoms to the cluster are pushed away from their initial positions, where the average distance between each Ni and its neighboring O_u is 1.8 Å as it was in Ni_2/ZrO_2(111) and Ni_3/ZrO_2(111).

Bader charge analysis shows that flat-Ni_4/ZrO_2(111) behaves similarly to Ni_2/ZrO_2(111) and Ni_3/ZrO_2(111): upon Ni_4 adsorption, the Ni_4 cluster becomes positively charged (+0.4 e), the negative charge of O_u (nearest neighbors of Ni) decreases by 0.1 e^- and the positive charge of Zr (nearest neighbor of Ni) decreases by +0.3 e. Thus, a charge transfer from the cluster to the surface is responsible for the electronic rearrangement of the surface atoms.

The electron density difference plot of Ni_4/ZrO_2(111) (Figure 3) shows an important accumulation of charge between the cluster and the nearest Zr belonging to the surface. We also note that the O_u atomic orbitals are well localized and pointing towards their respective Ni neighbor. Finally, a depletion of charge surrounding each Ni atom is observed.

The last cluster we have considered is Ni_5/ZrO_2(111). Again, we have considered two initial shapes for Ni_5/ZrO_2(111): flat and pyramidal. However, after geometry optimization, the flat Ni_5 configuration converged to a shape similar to the pyramid configuration (shown in Figure 2 (f)) with a clustering energy of 1.88 eV. Therefore, whatever the initial shape of the Ni_5 cluster, the 5 Ni adatoms tend to adopt a pyramid shape on top of the zirconia surface. The most stable pyramid shape found is shown in Figure 2 (f) and the clustering energy calculated for this configuration is 1.53 eV. Therefore, in the optimized structure of Ni_5, we have 4 Ni atoms exposing a (111) face to the zirconia surface and interacting with the O_u atoms. One Ni atom is positioned on top of the 4 Ni to form the pyramid. O_u atoms act like a trap for the cluster since in Ni_5/ZrO_2(111) the Ni interacting with O_u atoms are oriented toward them with an average distance of 1.8 Å and O_u are pushed away from their initial position, similarly to the previous configurations (Ni_4/ZrO_2(111), Ni_3/ZrO_2(111), Ni_2/ZrO_2(111) and Ni_1/ZrO_2(111)).

Bader charge analysis shows the same behavior as in the adsorption of the smaller clusters: the negative charge of O_u interacting with Ni decreases from –1.2 e^- to –1.1 e^- upon cluster adsorption; the positive charge of the Zr atom near the cluster decreases from 2.3 e^- to 2.0 e^-. Finally, the Ni_5 adsorbed cluster has a charge of +0.4 e explaining the electronic rearrangement observed in the zirconia atoms. The charge lost by the cluster is partially accumulated between the cluster and the surface and affects the electron localization of the surface atoms. The electron density difference plot of Ni_4/ZrO_2(111) (Figure 3) shows this charge accumulation between the cluster and the nearest Zr. It also shows the orientation of the O_u atomic orbitals, which are again localized and pointing towards Ni atoms.

3.2 Ni Diffusion on ZrO_2(111)

The general trend of the interaction of the five clusters (Ni_{1-5}) with the surface shows that the Ni atoms interact mainly with O_u and Zr. When the number of Ni in the cluster is > 2, the Ni cluster shape is a (111)-facet and the cluster is positioned in a way to maximize its interaction with O_u and Zr atoms. Figure 4 shows that the clustering energy is proportional to the size of the adsorbed Ni cluster: the larger the cluster, the lower E_{clus}, i.e. the trend of Ni clusters on ZrO_2(111) indicates that aggregation of the Ni atoms is preferred over dispersion of individual atoms across the surface.

Furthermore, we note from Table 1 that the difference between E_{clus} and E_{coh} decreases with the increase of the cluster size, due to the decrease of the ratio of interaction between metal atoms and the surface for larger clusters. Therefore, the cluster-surface interaction contributes weakly to the clustering energy. A similar result was found by Ma et al. [20] in their investigation of the adsorption of Ag clusters on the AgCl(100) surface.

E_{int} decreases with cluster size (Table 1) which is predictable since for larger clusters there are more atoms in contact with the surface, leading to an augmentation of perpendicular Ni-surface interactions. We also note from Table 1 that the d-band center decreases with the increase of the cluster size.

We have next evaluated the activation energy of diffusion of one Ni towards the Ni_4 cluster on top of ZrO_2(111) surface (Figure 5), by identifying the transition state along the diffusion pathway using the dimer method [41].

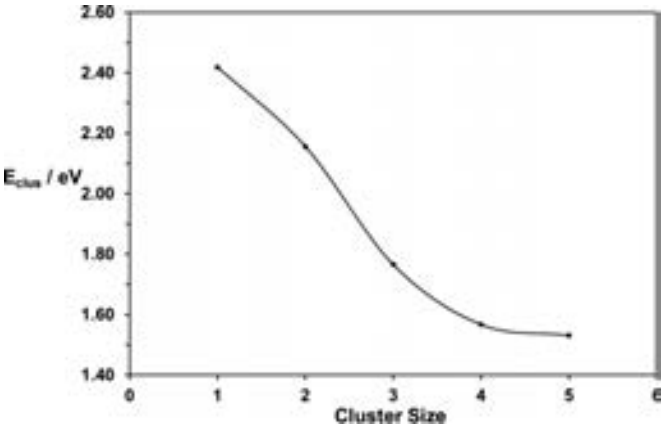

Fig. 4 Calculated clustering energy (E_{clus} / eV) for different cluster Ni_n adsorbed on ZrO_2(111). We show here the most stable structures.

 © 2017 The Authors. Published by WILEY-VCH Verlag GmbH & Co. KGaA, Weinheim

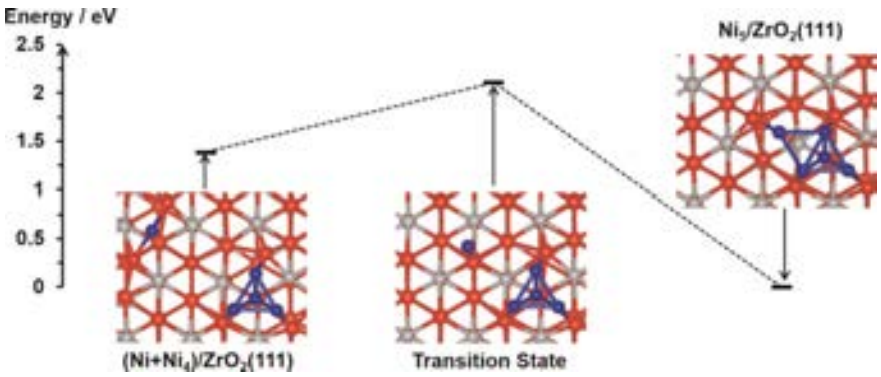

Fig. 5 Energy profile showing (Ni+Ni_4)/ZrO_2(111) and Ni_5/ZrO_2(111) states separated by a transition state. Color key: red, gray, and blue spheres correspond to oxygen, Zr and Ni atoms, respectively.

Figure 5 shows that the configuration Ni_5/ZrO_2(111) is more stable than (Ni+Ni_4)/ZrO_2(111), which indicates that the Ni atoms prefer to aggregate rather than be dispersed on the surface, which is in good agreement with the clustering energies calculated in the previous section. The energy difference between the transition state and (Ni+Ni_4)/ZrO_2(111) structures, i.e. the activation energy, is equal to 0.72 eV. Thus, using this activation energy (ΔE = 0.72 eV), we can calculate the hopping rate from state (Ni+Ni_4)/ZrO_2(111) to state Ni_5/ZrO_2(111) of the Ni atom: $k_{A\rightarrow B} = \nu \exp(\frac{-\Delta E}{k_B T})$ where A is state (Ni+Ni_4)/ZrO_2(111) and B is state Ni_5/ZrO_2(111). The Boltzmann constant k_B = 1.37789×10^{-5} eV K^{-1} and the vibrational frequency ν is approximately equal to 10^{12} s^{-1}. $k_{A\rightarrow B}$ is then calculated for a range of temperatures, corresponding to the working temperature of the SOFC (T = 500°C–900°C). Figure 6 shows that this $k_{A\rightarrow B}$ varies from 1.87×10^{7} to 7.66×10^{8} s^{-1}, indicating that Ni diffusion on the ZrO_2(111) surface occurs under the experimental conditions.

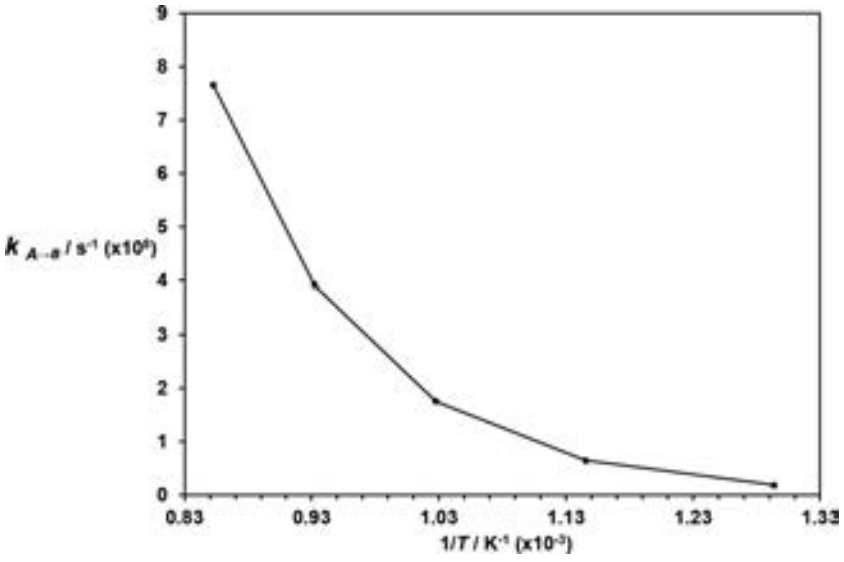

Fig. 6 Hopping rate for an Ni atom on ZrO_2(111).

4 Conclusions

We have studied the interaction of five Ni_n (n = 1–5) clusters with the ZrO_2(111) surface, where we have shown that the clustering energy decreases with increasing Ni cluster size. The clustering energy was positive for all clusters, indicating that Ni atoms prefer to aggregate rather than wet the surface. When the number of Ni in the cluster is > 2, the Ni cluster shape is a (111)-facet and the cluster is positioned in such a way to maximize its interaction with O_u and Zr atoms. From the electronic structure analysis (charges and electron density differences) we have demonstrated that Ni clusters transfer charge to the surface, which affects the electronic structure of O_u and Zr atoms: there is an accumulation of charge between Ni and the surface atoms and the atomic orbitals of O_u are well localized and point towards Ni. Finally, based on the results of clustering energy, diffusion barrier and hoping rates, it can be concluded that nucleation of clusters of Ni atoms can take place on the ZrO_2(111) surface under the experimental conditions specific to the applications of SOFC. A potential solution to clustering of the Ni particles may be the introduction of a dopant in order to trap the diffusing Ni atoms. We could also consider a reconstruction of the zirconia surface, as shown in the study by Tosoni et al. [42], where the authors showed that the adsorption of Ru on a step on the ZrO_2 surface is more stable than on a regular surface.

Acknowledgment

We acknowledge the Engineering and Physical Sciences Research Council (Grant nos. EP/K001329 and EP/K016288) for funding. ACE acknowledges the UCL Doctoral Training Centre in Molecular Modeling and Materials Science (EPSRC grant no. EP/G036675) for a studentship and NHdL acknowledges the Royal Society for an Industry Fellowship.

Via our membership of the UK's HPC Materials Chemistry Consortium, which is funded by EPSRC (EP/L000202), this work made use of the facilities of ARCHER, the UK's national high-performance computing service, which is funded by the Office of Science and Technology through EPSRC's High End Computing Programme. The authors also acknowledge the use of the UCL@Legion High Performance Computing

 © 2017 The Authors. Published by WILEY-VCH Verlag GmbH & Co. KGaA, Weinheim

Facility, and associated support services, in the completion of this work. Finally, the authors acknowledge the use of the IRIDIS High Performance Computing Facility, and associated support services at the University of Southampton, in the completion of this work.

References

[1] R. Grau-Crespo, N. C. Hernandez, J. F. Sanz, N. H. de Leeuw, *J. Phys. Chem. C* **2007**, *2*, 10448.
[2] C. R. A. Catlow, S. A. French, A. A. Sokol, M. Alfredsson, S. T. Bromley, *Faraday Discuss.* **2003**, *124*, 185.
[3] W. Wang, Z. Liang, X. Han, J. Chen, C. Xue, H. Zhao, *J. Alloys Compd.* **2015**, *622*, 504.
[4] V. E. Henrich, P. A. Cox, *The Surface Science of Metal Oxides*, Cambridge University Press, Cambridge, U.K., **1994**.
[5] M. Miyayama, K. Hikita, G. Uozumi, H. Yanagida, *Sensors Actuators B. Chem.* **1995**, *25*, 383.
[6] A. Y. Stakheev, L. . Kustov, *Appl. Catal. A Gen.* **1999**, *188*, 3.
[7] J. B. Goodenough, Y.-H. Huang, *J. Power Sources* **2007**, *173*, 1.
[8] P. I. Cowin, C. T. G. Petit, R. Lan, J. T. S. Irvine, S. Tao, *Adv. Energy Mater.* **2011**, *1*, 314.
[9] B. C. H. Steele, A. Heinzel, *Nature* **2001**, *414*, 345.
[10] A. J. Jacobson, *Chem. Mater.* **2010**, *22*, 660.
[11] C. Sun, R. Hui, J. Roller, *J. Solid State Electrochem.* **2009**, *14*, 1125.
[12] S. Kim, H. Moon, S. Hyun, J. Moon, J. Kim, H. Lee, *Solid State Ionics* **2007**, *178*, 1304.
[13] N. Q. Minh, *J. Am. Ceram. Soc.* **1993**, *76*, 563.
[14] S. Kim, H. Moon, S. Hyun, J. Moon, J. Kim, H. Lee, *Solid State Ionics* **2006**, *177*, 931.
[15] B.-T. Teng, F.-M. Wu, W.-X. Huang, X.-D. Wen, L.-H. Zhao, M.-F. Luo, *Chemphyschem* **2012**, *13*, 1261.
[16] Z. Li, C. V. Ciobanu, J. Hu, J.-P. Palomares-Báez, J.-L. Rodríguez-López, R. Richards, *Phys. Chem. Chem. Phys.* **2011**, *13*, 2582.
[17] D. Jiang, S. H. Overbury, S. Dai, *J. Phys. Chem. C* **2012**, *116*, 21880.
[18] P. Luches, F. Pagliuca, S. Valeri, F. Illas, G. Preda, G. Pacchioni, *J. Phys. Chem. C* **2012**, *116*, 1122.
[19] K. R. Hahn, A. P. Seitsonen, M. Iannuzzi, J. Hutter, *ChemCatChem* **2015**, *7*, 625.
[20] X. Ma, Y. Dai, M. Guo, Y. Zhu, B. Huang, *Phys. Chem. Chem. Phys.* **2013**, *15*, 8722.
[21] C. Jung, H. Tsuboi, M. Koyama, M. Kubo, E. Broclawik, A. Miyamoto, *Catal. Today* **2006**, *111*, 322.
[22] P. Hohenberg, W. Kohn, *Phys. Rev.* **1964**, *136*, B864.
[23] G. Kresse, J. Furthmüller, *Phys. Rev. B – Condens. Matter Mater. Phys.* **1996**, *54*, 11169.
[24] G. Kresse, J. Furthmüller, *Comput. Mater. Sci.* **1996**, *6*, 15.
[25] G. Kresse, J. Hafner, *Phys. Rev. B* **1993**, *48*, 13115.
[26] G. Kresse, J. Hafner, *J. Phys. Condens. Matter* **1994**, *6*, 8245.
[27] J. P. Perdew, K. Burke, M. Ernzerhof, *Phys. Rev. Lett.* **1996**, *77*, 3865.
[28] S. Grimme, *J. Comput. Chem.* **2006**, *27*, 1787. DOI: 10.1002/jcc.20495
[29] P. E. Blöchl, *Phys. Rev. B* **1994**, *50*, 17953.
[30] G. W. Watson, E. T. Kelsey, N. H. de Leeuw, D. J. Harris, S. C. Parker, *J. Chem. Soc. Faraday Trans.* **1996**, *92*, 433.
[31] D. Santos-Carballal, A. Roldan, R. Grau-Crespo, N. H. de Leeuw, *Phys. Chem. Chem. Phys.* **2014**, *16*, 21082.
[32] A. Cadi-Essadek, A. Roldan, N. H. de Leeuw, *J. Phys. Chem. C* **2015**, *119*, 6581.
[33] G. Stapper, M. Bernasconi, N. Nicoloso, M. Parrinello, *Phys. Rev. B* **1999**, *59*, 797.
[34] X. Xia, R. Oldman, R. Catlow, *Chem. Mater.* **2009**, *21*, 3576.
[35] R. Grau-Crespo, N. C. Hernández, J. F. Sanz, N. H. de Leeuw, *J. Mater. Chem.* **2009**, *19*, 710.
[36] H. R. Chauke, P. Murovhi, P. E. Ngoepe, N. H. de Leeuw, R. Grau-Crespo, *J. Phys. Chem. C* **2010**, *114*, 15403.
[37] F. Grau-Crespo, R. Catlow, C. R. A. de Leeuw, N. H. Neyman, K. Illas, *Sci. Supercomput. Eur.* **2007**, 166.
[38] Y. Liu, Y. Wang, G. Chen, *J. Mol. Model.* **2011**, *17*, 1061.
[39] J. Li, E. Croiset, L. Ricardez-Sandoval, *Phys. Chem. Chem. Phys.* **2014**, *16*, 2954.
[40] S. Hong, Y.-H. Shin, J. Ihm, *Jpn. J. Appl. Phys.* **2002**, *41*, 6142.
[41] A. Heyden, A. T. Bell, F. J. Keil, *J. Chem. Phys.* **2005**, *123*, 224101.
[42] S. Tosoni, H.-Y. T. Chen, G. Pacchioni, *Chem. Phys. Chem.* **2015**, *16*, 3642.

 © 2017 The Authors. Published by WILEY-VCH Verlag GmbH & Co. KGaA, Weinheim